Cell Reports, Volume *21*

Supplemental Information

Functional Plasticity of Odor Representations during Motherhood

Amit Vinograd, Yael Fuchs-Shlomai, Merav Stern, Diptendu Mukherjee, Yuan Gao, Ami Citri, Ian Davison, and Adi Mizrahi

Supplemental experimental procedures

Immunohistochemistry and confocal microscopy For visualization of MCs in confocal microscopy (Fig. 1A), we perfused mice transcardially with PBS, followed by 4% paraformaldehyde and cryoprotected the brain in 30% sucrose overnight. We sectioned OBs coronally on a sliding microtome (40 µm slices), washed the slices in PBS and then incubated them for 2 hours in a blocking solution (5% normal goat serum and 0.4% Triton-X). We incubated slices overnight at room temperature with primary antibodies diluted in the blocking solution (rabbit anti-GFP, Millipore 1:1000) washed them in PBS, and then incubated them for 2 hrs at room temperature with secondary antibodies (Jackson ImmunoResearch), diluted 1:500 in the blocking solution (DyLight488-conjugated goat anti-rabbit). Prior to mounting on microscope slides, we incubated the slices with DAPI (Santa Cruz Biotechnology; 50µg/ml) for 5 min and then washed them with PBS. We obtained confocal images using a Leica SP-5 confocal microscope, using a 40X (1.3 NA) oil objective.

Data analysis Change index (Fig. S1B, S1D, S1F, S1H) was calculated as follows: $\frac{\sum_{n=1}^{number\ of\ odors}(\frac{Mother_n}{Naive_n}-1)}{number\ of\ odors}$ where $Mother_n/Naive_n$ are the values for each odor either for response amplitude (Fig. S1B,S1D) or responsiveness (Fig. S1F, S1H).

For mixture processing analysis (Fig. 4) we calculated the mixture change by subtracting the peak amplitude of the mixture from the strongest activating odor on all responsive cells. Repeating the analysis on all cells, on only responsive to 2 odors and by subtracting the weakest activating odor resulted with qualitatively the same result. For pairwise correlation (Fig. 7E), we calculated the pearson correlation of the maximum ΔF/F in responsive cells between all pairs in each recorded field of the same animal.

The ensemble activity response of MCs to a given odor at each time point was expressed as a vector $\bar{V}_\alpha$, where α denotes the odor and each component i of the vector is the activity of cell i in response to the odor at that time point. Only cells that responded to at

least one odor were included in the ensemble vectors. To evaluate how similar responses to different odors are in cell activities space, we took the response vectors and calculated the cosine similarity between them (see illustrations in Figure 7F):

$$\text{Cosine similarity} = \frac{\sum_{i=1}^{n}(V_{i,\alpha}V_{i,\beta})}{\sqrt{\sum_{i=1}^{n}(V_{i,\alpha})^2}\sqrt{\sum_{i=1}^{n}(V_{i,\beta})^2}}$$

To evaluate how far responses to different odors are in cell activities space, we took the response vectors and calculated the Euclidean distance. We accounted for the different number of cells responding in each population with a normalization factor. The formula is given by:

$$Euclidean\ distance = \frac{1}{\sqrt{n}}\sqrt{\sum_{i=1}^{n}\left(V_{i,\alpha} - V_{i,\beta}\right)^2}$$

with n the number of responding cells (to any odor) which is the number of dimensions contributing to the activity in space. This measure is sensitive to the relative magnitude of the responses and describes the distance in space between them. An intuition to this measure is also given by the separation of the first three principle components of the different odors (Fig. 7I). The visual distances between the principle components of each odor is what is actually measured in Fig. 7G,H with the only exception that instead of using only the first three dimensions (restricted by a plot) we use the full responding cell activities space. Since our main goal was to compare the distribution of separation of odor pairs between mothers and naïve (pure vs. natural) we normalized the resulting distances by dividing all odor pairs in mothers according to the largest odor pair distance received in mothers and the same for all odor pairs in naïve according to the largest odor pair in naïve.

Odor delivery

To deliver odorants we used a custom-made 11 channels olfactometer. In order to avoid cross-contamination between odorants we used separate tubing for each channel, all the

way from the odor vial to the animal's nose. For pure odors we used a panel of 6 odorants known to activate different and partially overlapping areas in the dorsal part of the OB (butanal, pentanal, ethyl-tiglate, propanal, methyl-propionate, ethyl-butyrate and ethyl-acetate; all obtained from Sigma-Aldrich, St. Louis, MO). We presented each pure odorant at a final concentration of 50 ppm, for 2 and 15 seconds with a 15 second inter-stimulus interval, repeated for 4 times, in pseudo-random order. Each repeat included a blank trial consisting of all components of a standard trial, except for odor presentation. For a subset of mice we added to the 6 pure odorants 5 natural odorants- male urine, female urine, peanut butter, trimethylthiazoline (TMT) and nest odor. Urine was collected from thy1-GCaMP3 males and females and stored at -20°c. 10µl was placed in the odor vials. Peanut butter was made of 100% peanuts (Better&different, Mishor Edomim, Israel) and 1gr peanut butter was placed in the vials. For predator odor we used 1µl of TMT (Contech, Delta, Canada). Nest odor was made of 0.5gr nest bedding and 1 pup that was kept warm using a heating pad. For mixtures experiment we used ethyl-acetate methyl-propionate ethyl-tiglate and their mixtures where combined via air in front of the mouse nose. In anesthetized mice, in order to trigger the odor delivery at the onset of inhalation, we monitored the animal's respiration throughout the experiment by a low pressure sensor (1-INCH-D1-4V-MINI, 'All sensors', Morgan Hill, CA). We connected the low pressure sensor to a thin stainless steel tubing (OD 0.7 mm) and placed it at the entrance of the animals' contra-lateral nostril. The information from the pressure sensor was passed to an analogue converter (window discriminator), which we used to identify the inhalation onset during the respiratory cycle. Each odor stimulus was triggered at onset of inhalation.

RNA extraction, cDNA preparation and quantitative PCR

OBs were collected as quickly as possible (normally in less than 2 min) in ice-cold conditions in a clean and RNase free environment, transferred immediately to Tri-Reagent (Sigma) and stored at -80°C until homogenization. Tissue was homogenized using a 25G long needle and RNA was extracted. RNA concentration was determined by a nanodrop spectrophotometer and 300ng of RNA was used for random-primer based

cDNA preparation (Applied Biosystems, High Capacity cDNA Reverse Transcription Kit). cDNA was diluted to 2ng/µl and processed for qPCR analysis using SYBR Green probes in a Light-cycler® 480 Real Time PCR Instrument (Roche Light Cycler*480 SYBR Green I Master). Relative levels of gene expression (ΔCt) were obtained by normalizing gene expression to a housekeeping gene (GAPDH). Fold induction was calculated using the ΔΔCt method, addressing fold induction of OBs from mothers in comparison to OBs from naïve females. Statistical analysis was performed using Excel. Primers were ordered from IDT DNA. A list of primers used and their efficiency is included in supplementary table 1.

Slice electrophysiology

Sagittal brain slices (300 µm thick) were prepared from the main olfactory bulb of lactating mothers C57Bl6/J mice, 3-5 days after parturition (11-14 weeks of age) using a Leica VT1200S vibratome. All animals had litters of ≥3 pups and displayed appropriate maternal care. Control recordings were carried out from group-housed,age-matched females. To obtain viable slices from adult animals, mice were anesthetized with ketamine/xylazine and transcardially perfused with protective artificial cerebrospinal fluid (ACSF) containing, in mM: 124 NaCl, 2.5 KCl, 1.25 NaH_2PO_4, 25 $NaHCO_3$, 75 sucrose, 10 glucose, 1.3 ascorbic acid, 0.5 $CaCl_2$ and 7 $MgCl_2$. Slices were incubated and recorded using standard ACSF containing, in mM: 124 NaCl, 3 KCl, 1.25 NaH_2PO_4, 26 $NaHCO_3$, 20 D-glucose, 2 $CaCl_2$ and 1.5 $MgCl_2$, continuously oxygenated with 95% CO_2 / 5% O_2. Whole cell voltage clamp recordings of mitral cells were carried out at 29.5oC in a submerged recording chamber. Slices were visualized with Dodt contrast using a two-photon imaging system (Prairie Technologies Ultima) and Alexa594 was added to the internal solution to confirm cell type and intact dendritic arbor. For electrical stimulation, glass stimulation pipettes were placed adjacent to the cell's parent glomerulus and the olfactory nerve was stimulated with brief current pulses (0.2ms, 4-12 µA; 120% of threshold). Voltage clamp recordings of miniature synaptic currents were made with high-Cl- internal solutions containing, in mM: 115 CsCl, 25 TEA-Cl, 5 QX314-Cl, 0.2 EGTA, 4 MgATP, 0.3 Na_3GTP and 10 phosphocreatine disodium. Evoked excitatory / inhibitory synaptic currents were recorded with internal solutions

containing, in mM: 130 Cs Methanesulfonate, 4 NaCl, 10 HEPEs, 1 EGTA (pH with CsOH), 4 MgATP, 0.3 Na3GTP, 10 Phosphocreatine disodium, 25 TEA-OH, 5 QX314-Cl. Electrophysiological data were acquired at 10 KHz using a Multiclamp 700B amplifier (Molecular Devices, Sunnyvale, CA), data acquisition board (USB 1221, National Instruments), and custom MATLAB routines (Mathworks, Natick, MA). Inhibitory events were detected and quantified using Igor Pro (WaveMetrics, Lake Oswego, Oregon).

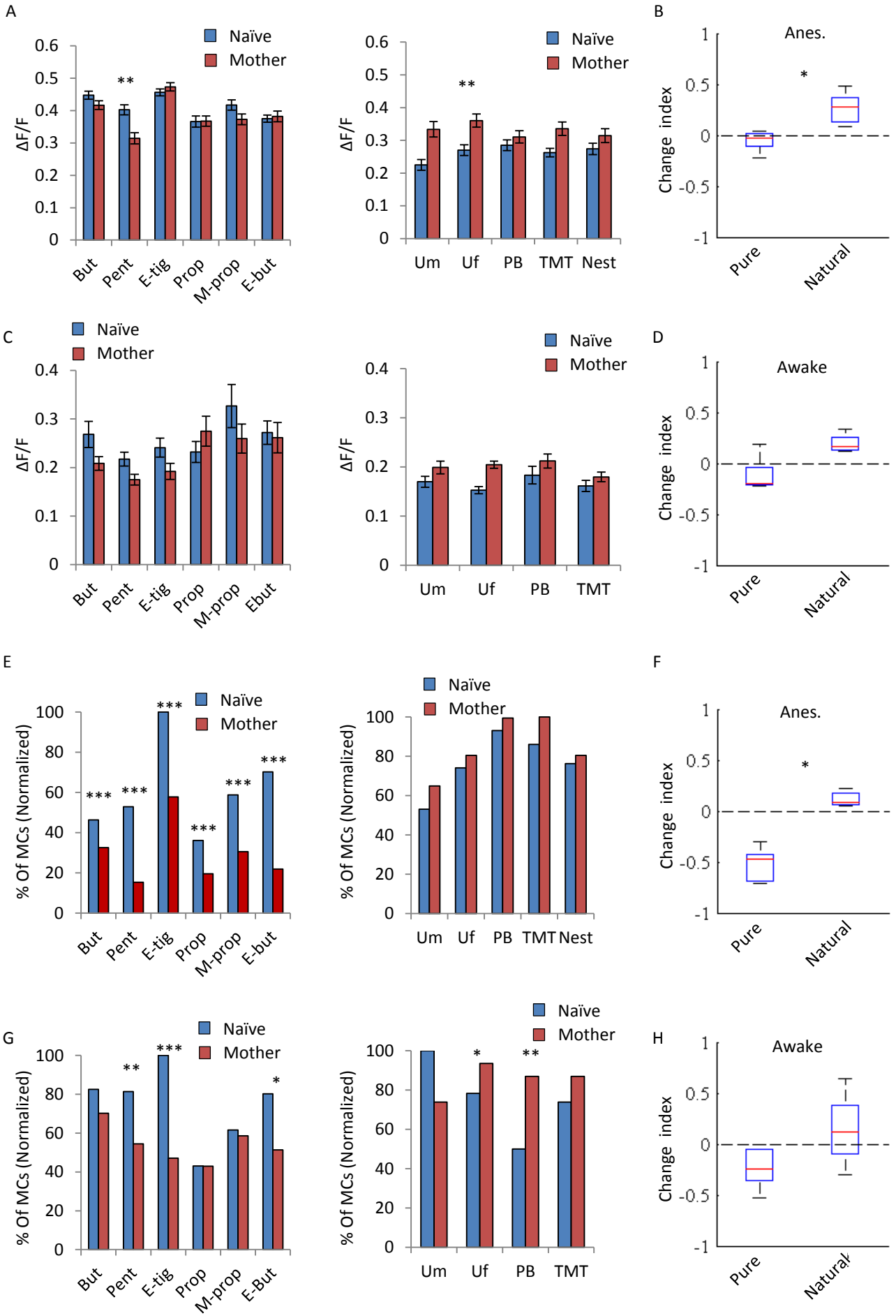
A
Naïve
Mother
ΔF/F
But
Pent
E-tig
Prop
M-prop
E-but
Um
Uf
PB
TMT
Nest
B
Anes.
Change index
Pure
Natural
C
Ebut
D
Awake
E
% Of MCs (Normalized)
F
G
E-But
H

Figure S1

Fig. S1. Analysis per-odor shows increased sparsening to pure odors and higher responsiveness to natural odors, related to Figure 1, 2 and 3. (A) Left - Average ΔF/F response values to the different pure odors in anesthetized Naïve females (blue) and Mothers (red). Black error bars- SEM. Right - same as 'A' for natural odors. **(B)** Change index of average ΔF/F response values between Naïve females and Mothers for pure and natural odors. In each box, red lines represent the median, edges are the 25th and 75th percentiles, top and bottom bars show the most extreme data points. **(C-D)** Same as A-B but for awake mice. **(E)** Left - Percentage of cells responding to each individual pure odor normalized to the most responsive odor. Blue bars- Naïve females, red- Mothers. Right - Same as 'D' but for natural odors. **(E)** Change index of responsiveness values between naïve females and mothers for pure and natural odors. **(G-H)** Same as E-F but for awake mice. (*p<0.05, **p<0.001, ***p<0.0001, A,C-binomial proportion test, B,D,E,F,G,H - Mann-Whitney U test).

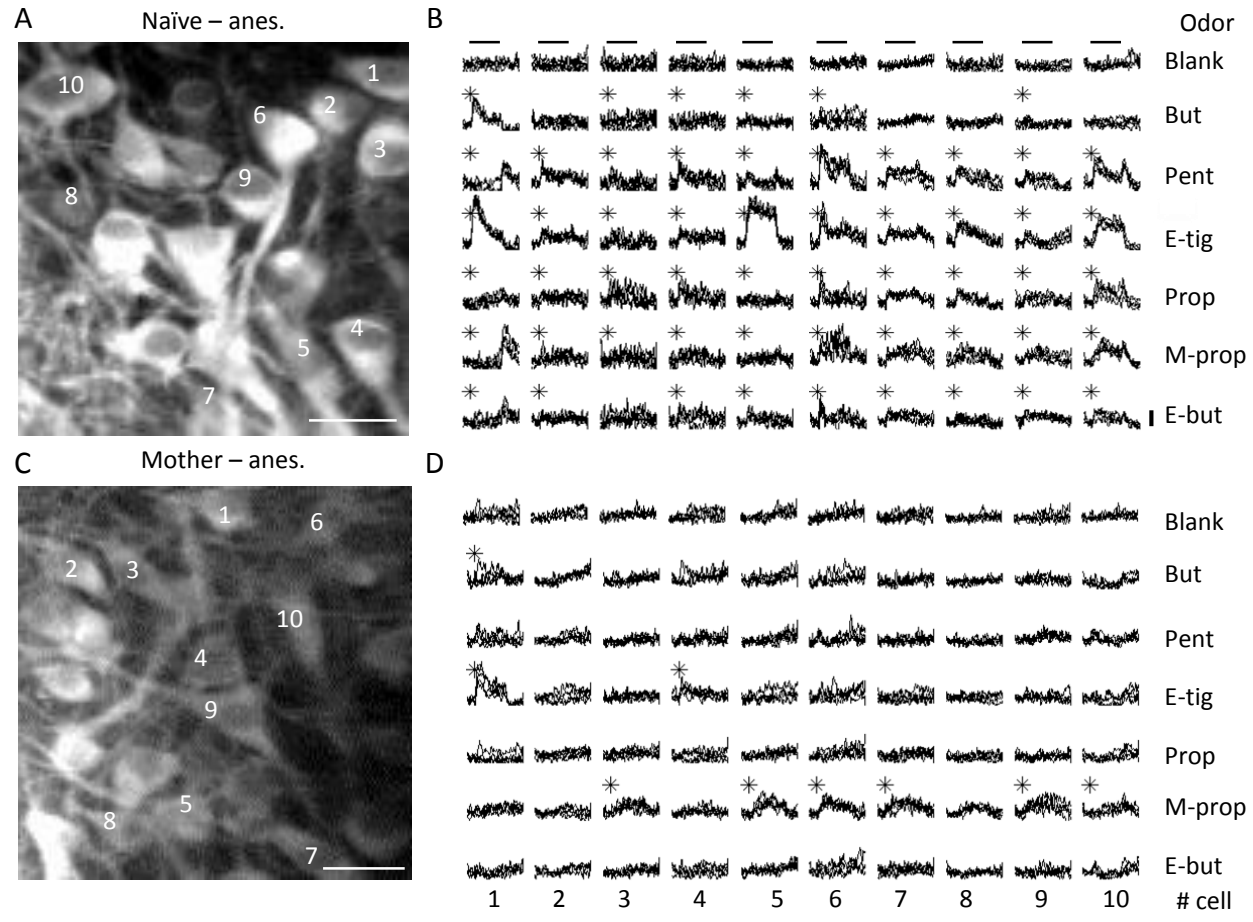
A
Naïve – anes.
10
1
6
2
3
8
9
5
4
7
B
Odor
Blank
But
Pent
E-tig
Prop
M-prop
E-but
C
Mother – anes.
1
6
2
3
10
4
9
8
5
7
D
Blank
But
Pent
E-tig
Prop
M-prop
E-but
1 2 3 4 5 6 7 8 9 10
cell

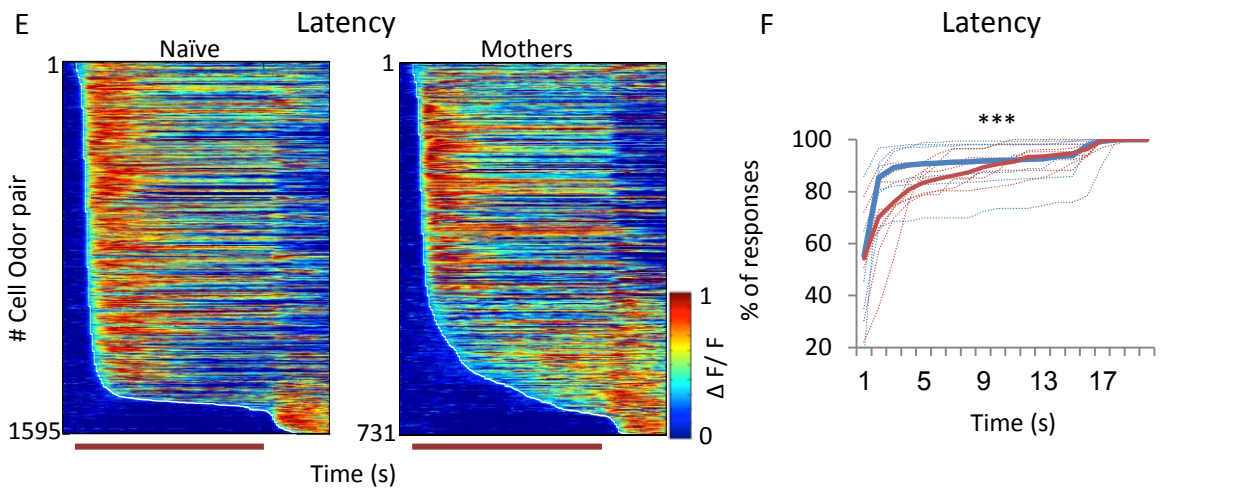
E
Latency
Naïve
Mothers
1
1595
731
Cell Odor pair
Time (s)
1
0
Δ F/ F
F
Latency
***
100
80
60
40
20
% of responses
1 5 9 13 17
Time (s)

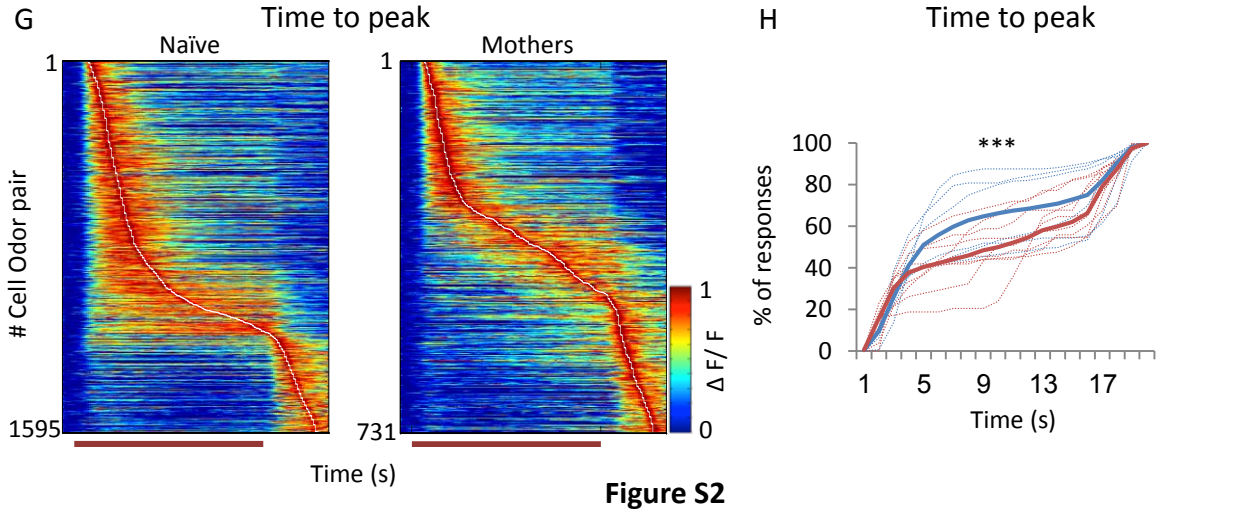
G
Time to peak
Naïve
Mothers
1
1595
731
Cell Odor pair
Time (s)
1
0
Δ F/ F
H
Time to peak
***
100
80
60
40
20
0
% of responses
1 5 9 13 17
Time (s)

Figure S2

- **Fig. S2. Changes in MC responses to persistent odor stimulation in mothers, related to Figure 1. (A)** Two photon micrograph of a representative field used for imaging in a naïve female. Scale bar, 20μm. **(B)** Calcium transients elicited by the neurons in the field shown in A (cells marked by numbers in A) in response to a 15 second odor stimulation with 6 odors. Each line represents a single trial. Black asterisk denotes a statistically significant response. Vertical bar - 25% ΔF/F. **(C-D)** As in 'A-B' but example from a mother. **(E)** Time course for all the responsive cell-odor pairs in naïve females (left panel) and mothers (right panel) normalized to the peak response and sorted by latency to respond. Horizontal line denotes odor stimulation (15 seconds). **(F)** Cumulative distribution of response latency of all the responsive cell-odor pairs in naïve females (blue) and mothers (red) ($p<0.0001$, Kolmogorov-Smirnov test). Each dashed line represents an individual mouse**. (G)** As in 'E' but data sorted by time to peak. **(H)** As in 'F' but for values of time to peak ($p<0.0001$, Kolmogorov-Smirnov test).

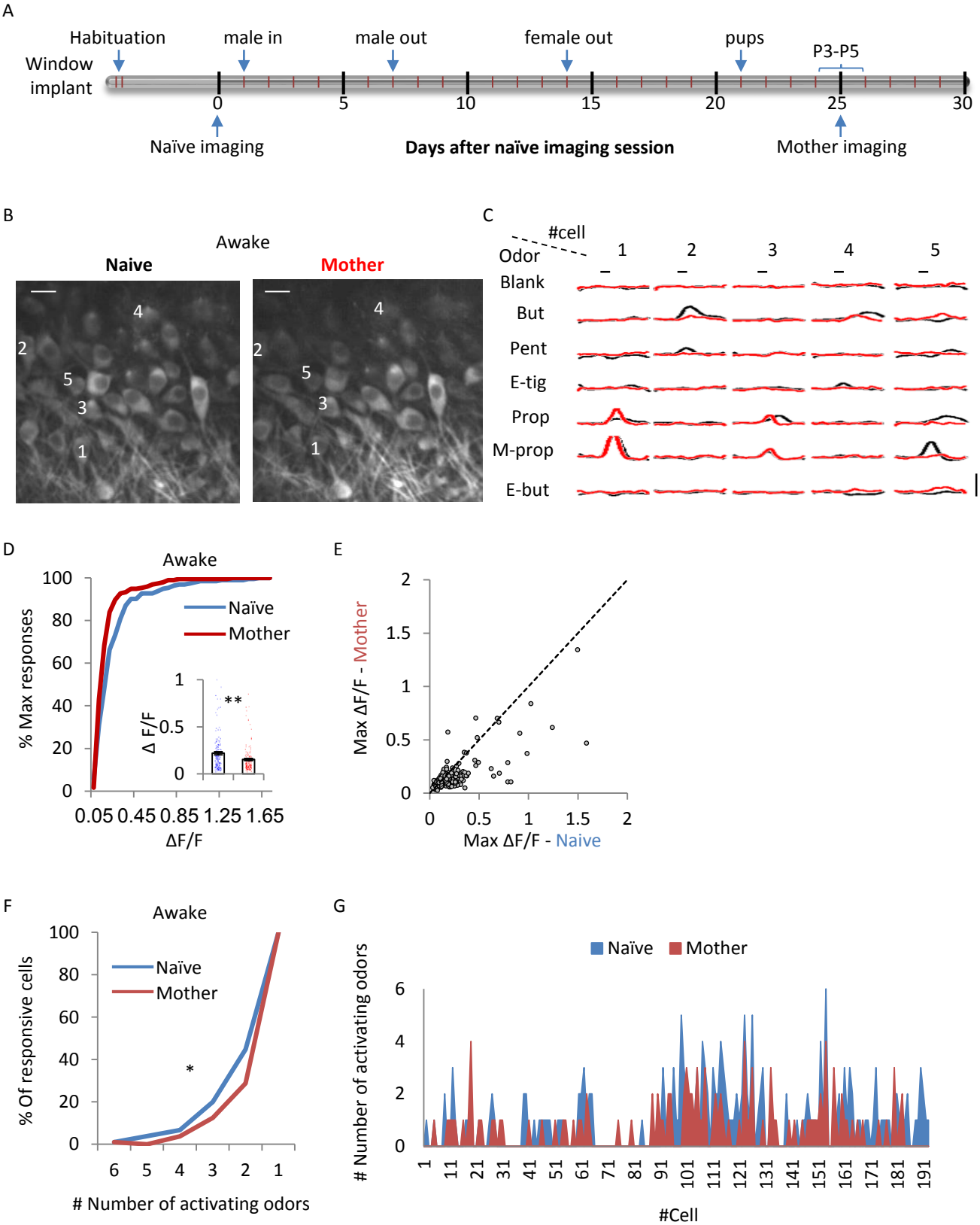
A
Habituation
male in
male out
female out
pups
P3-P5
Window implant
0
5
10
15
20
25
30
Naïve imaging
Days after naïve imaging session
Mother imaging
B
Awake
Naive
Mother
C
#cell
Odor
1
2
3
4
5
Blank
But
Pent
E-tig
Prop
M-prop
E-but
D
Awake
Naïve
Mother
% Max responses
Δ F/F
**
ΔF/F
E
Max ΔF/F - Mother
Max ΔF/F - Naive
F
Awake
Naïve
Mother
% Of responsive cells
*
Number of activating odors
G
Naïve
Mother
Number of activating odors
#Cell

Figure S3

Fig. S3. Time lapse imaging of MCs supports the sparsening of MCs in mothers, related to Figure 2. (A) Experimental timeline. **(B)** Two photon micrograph of a representative field showing the same MCs before (left) and after (right) parturition. Scale bar, 20μm. **(C)** Calcium transients elicited by 5 neurons in the field shown in 'B' in response to a 2 seconds odor stimulation with 6 odors. Each trace represents a mean of 4 trials. Black – naïve females, red - mothers. Vertical bar - 25% ΔF/F. **(D)** Cumulative distribution of peak odor evoked responses before (blue) and after (red) parturition. Inset: Mean±SEM peak amplitude of odor-evoked calcium transients per cell before (blue) and after (red) parturition (**P<0.001, Mann-Whitney U test). **(E)** Max ΔF/F of all individual MCs before (horizontal axis) and after (vertical axis) parturition. **(F)** Cumulative distribution of the percentage of MCs responding to 1-6 odors before (blue) and after (red) parturition (*P<0.01, Kolmogorov-Smirnov test). **(G)** Odor responsiveness in all individual MCs recorded before (blue) and after (red) parturition (n=193 cells).

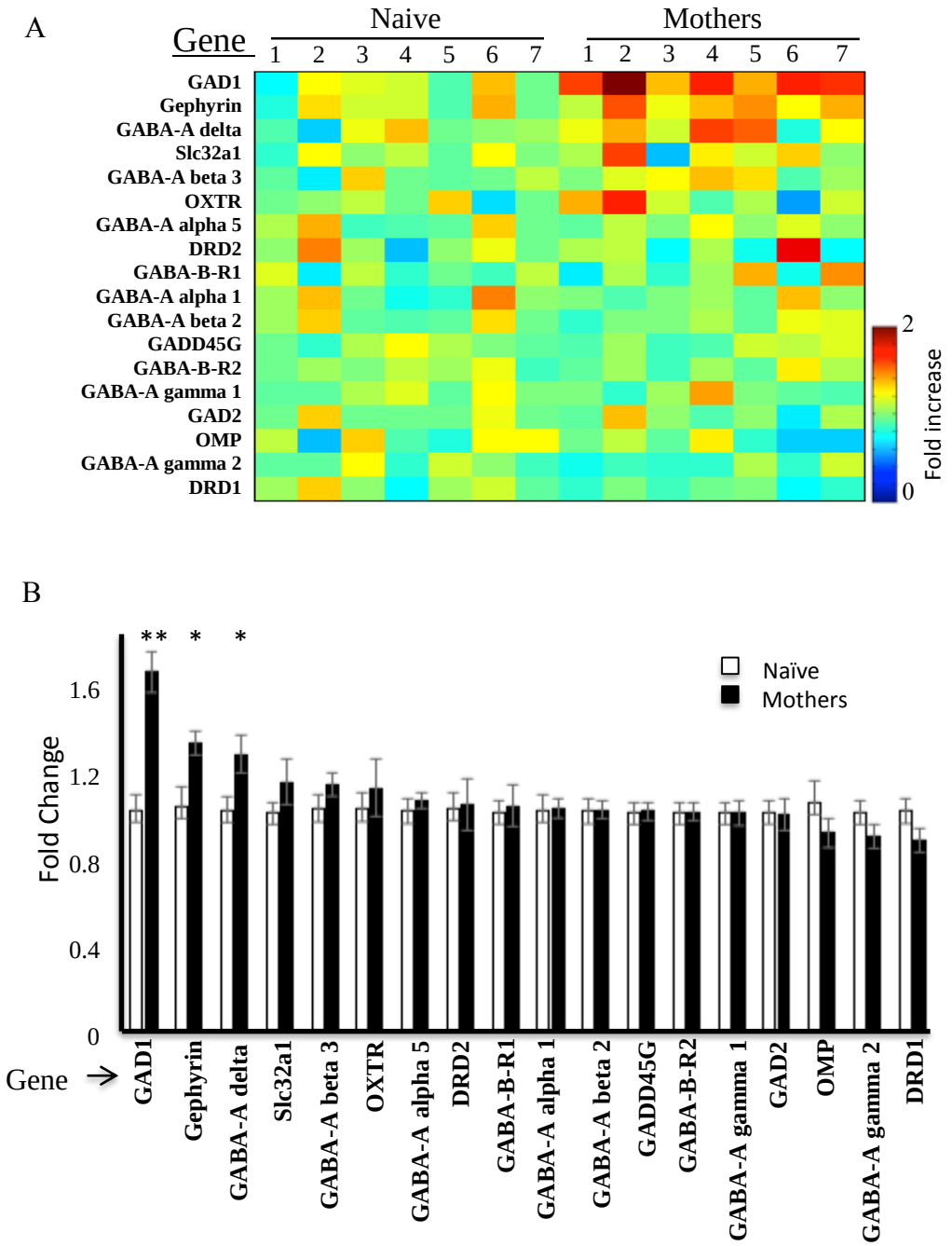
A
Gene
Naive
Mothers
1 2 3 4 5 6 7 1 2 3 4 5 6 7
GAD1
Gephyrin
GABA-A delta
Slc32a1
GABA-A beta 3
OXTR
GABA-A alpha 5
DRD2
GABA-B-R1
GABA-A alpha 1
GABA-A beta 2
GADD45G
GABA-B-R2
GABA-A gamma 1
GAD2
OMP
GABA-A gamma 2
DRD1
2
0
Fold increase
B
Naïve
Mothers
Fold Change
1.6
1.2
0.8
0.4
0
** * *
Gene
GAD1
Gephyrin
GABA-A delta
Slc32a1
GABA-A beta 3
OXTR
GABA-A alpha 5
DRD2
GABA-B-R1
GABA-A alpha 1
GABA-A beta 2
GADD45G
GABA-B-R2
GABA-A gamma 1
GAD2
OMP
GABA-A gamma 2
DRD1

Figure S4

Fig. S4. Increase in GABA signaling pathway genes support increased inhibition in the OB of mothers, related to Figure 6. (A) Heat-map comparing the expression level of genes in individual mice from either Naïve females or Mothers (each pixel is an average of two independently assayed OBs in individual mice). Levels of comparative expression are represented as fold over the average of control. Data is sorted by the level of change in mothers vs naïve (top: highest change). **(B)** Fold induction of the selected genes, comparing average (±SEM) gene expression in the OBs of naïve females and mothers. Statistically significant transcriptional upregulation was observed for GAD67, Gephyrin and GABAA-delta (**p< 0.001 and *p< 0.05, T-test).

Gene name:	Gene abbreviation	Forward Primer	Reverse Primer	% Efficiency
dopamine receptor D1	*Drd1*	acaacggggctgtgatgt	catgagggatcaggtaaacca	102.5
dopamine receptor D2	*Drd2*	tgaacaggcggagaatgg	ctggtgcttgacagcatctc	103.8
gamma-aminobutyric acid type A receptor delta subunit	*Gabrd*	caaggtcaaggtcaccaagc	gggagatagccaactcctga	97.5
gamma-aminobutyric acid type A receptor gamma1 subunit	*Gabrg1*	gaggcaggaagctgaaaaac	tgctgttcatgggaatgaga	101.2
gamma-aminobutyric acid type A receptor gamma2 subunit	*Gabrg2*	ggaatacaactgaagtagtgaagacaa	ttctgctcagatcgaagtacaca	101.6
gamma aminobutyric acid type A receptor alpha1 subunit	*Gabra1*	gcccactaaaattcggaagc	cttctgctacaaccactgaacg	98.1
gamma aminobutyric acid type A receptor alpha5 subunit	*Gabra5*	gacggactcttggatggcta	acctgcgtgattcgctct	99.3
gamma aminobutyric acid type A receptor beta2 subunit	*Gabrb2*	caatatccacgtaggtagagaacact	ttctacatggactgctatttctgg	104.1
gamma aminobutyric acid type A receptor beta3 subunit	*Gabrb3*	ggattgttctcgtaggaataggc	gaaatgaaatcgacgggaatac	108.0
gamma aminobutyric acid type B receptor subunit 1	*Gabbr1*	gctccaagaagatgaatacatgg	ttttggtctcataagcaagaaaga	99.6
gamma aminobutyric acid type B receptor subunit 2	*Gabbr2*	aggtgaaggtcggcgagta	tggtgtcgttgatgatctcc	105.1
gephyrin	*Gphn*	tgatcttcatgctcagatcca	gcaaatgttgttggcaagc	101.7
glutamate decarboxylase 2	*Gad2*	tttccagaagtcaaggagaagg	cagctcccttcttgagagaaaa	102.6
glutamate decarboxylase 1	*Gad1*	tggagatgcgaaccatgag	gaagggttcctggtttagcc	105.8
growth arrest and DNA damage inducible gamma	*Gadd45g*	ggataacttgctgttcgtgga	aagttcgtgcagtgctttcc	102.5
olfactory marker protein	*Omp*	acagctttagagacccctttgg	atccgagtgaggcagagttg	107.9
oxytocin receptor	*Oxtr*	acttagggcaagctggttga	cctgggtccaaaaatgacac	98.5
solute carrier family 32 member 1	*Slc32a1*	tgagggtggccagatttc	cctcctgctaaaccatgacc	103.6

Supplemental table 1. Genes, primer sequences and primer efficiency calculation, related to Fig.S4.